Sub-thrust imaging over the Timor Trough using broadband seismic, full waveform inversion and fault constrained tomography

Yonghe Guo and Shiping Wu, CGG; Masamichi Fujimoto and Yuki Sasaki, INPEX*

Summary

Sub-thrust imaging in the Timor Trough suffers from fault shadows caused by strong lateral velocity variations. Here we demonstrate a new workflow to tackle this problem. Broadband seismic data were acquired with a high signal-to-noise (S/N) ratio at the low frequencies. With broadband input, full waveform inversion (FWI) derived a better velocity model in the shallow thrust area where reflection tomography has limitations. Compared to conventional tomography, which has difficulty in addressing sharp velocity boundaries properly, fault constrained tomography (FCT) uses the interpreted fault planes as a constraint in the inversion, and benefits from better low frequency penetration in the severe fault shadows. Broadband seismic and depth imaging with FWI and FCT make a step change over the sub-thrust areas.

Introduction

This case study is from a project in East Indonesia which was carried out from 2013 to early 2014. The block is located in the Timor Trough, which was developed by the subduction between the Sunda and Australia plates. As shown on Figure 1, the target Mesozoic layer (green and yellow layers) is buried under the fold and thrust belt of thick Cenozoic carbonates developed in the foreland of the collisional zone. The water depth varies from 200 m to 2000 m and the deep target layer lies at 4-6 km. The legacy seismic image has severe fault shadow problems due to strong lateral velocity variations and poor low-frequency content of the data, which limits the imaging penetration in the thrust area. These are the major challenges to overcome in order to better understand the petroleum system and evaluate the risks of the exploration target. With these goals in mind, broadband seismic acquisition was chosen for its good low frequency data to improve long-wavelength imaging penetration. FWI and FCT were then employed to resolve the velocity variation across both the shallow and deep portions, both of which benefit from the extended bandwidth of the broadband seismic.

Broadband Seismic

3D broadband seismic data was acquired in early 2013. A cable length of 7050 m was selected to image the deep target using a variable-depth profile from 6 m to 50 m to provide optimized ghost diversity (Soubaras and Dowle, 2010). Ghost Wavefield Elimination (GWE) was then applied pre-stack to effectively remove the receiver ghost (Wang and Peng, 2013) and to provide a much wider bandwidth with enhanced high and low frequency content.

A pre-stack time migration (PSTM) stack of the broadband data and frequency panels are shown on Figure 2. As expected, the broadband variable-depth streamer data exhibit a high S/N ratio even for the very low frequencies (2-4 Hz). It is also observed that the 2-4 Hz energy penetrates down to 5-6 seconds while higher frequencies are absorbed more at this target level. Although the PSTM

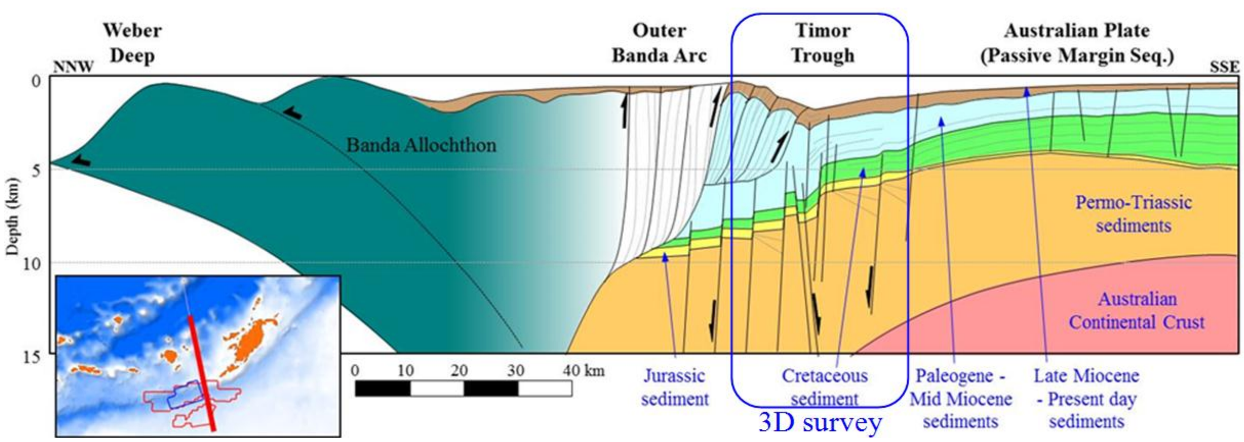

Figure 1: Schematic SSE to NNW regional section across the study area. The Mesozoic target is indicated by the green and yellow layers. The blue box indicates the approximate coverage of the 3D seismic with respect to the structure. The inset map shows the orientation of the schematic cross section.

DOI http://dx.doi.org/10.1190/segam2015-5841904.1

image is quite distorted near the fault and at the target level (highlighted on Figure 2), it is expected that the presence of the strong low frequency content in the broadband data will help to obtain an improved pre-stack depth migration (PSDM) result.

Full Waveform Inversion

Residual curvature picking in common image gathers (CIGs) can be extremely challenging in the shallow water thrust area. This is due, firstly, to the steep dip of the reflectors and, secondly, to that the reflected energy appears limited only to the near offsets. Hence reflection tomography gives a poor velocity update in this area.

FWI makes use of mainly transmitted energy and does not require CIGs, so it can produce much more accurate velocity models in the shallow areas. Since the initial model used as the input to FWI is not accurate in our case, low frequency energy is critical for FWI to avoid cycle skipping. In this case study, the combination of the good low frequency content and long offset information (up to 7 km) contained in this broadband data made FWI robust in spite of a poor initial velocity model in the shallow water thrust area.

Figure 3 compares the initial and FWI velocity model, with corresponding PSDM stack overlays. FWI was run in cascaded passes starting at [2.5, 4] Hz and ending at [2.5, 12] Hz in 1-Hz increments. The FWI velocity model has a much higher resolution and matches the folded structures in the thrust zone very well. As indicated by the left arrow, the seismic image is over-migrated before FWI but more focused after FWI. At the middle arrow, structures cross each other before FWI and move to the correct position after FWI. As indicated by the right (double-headed) arrow, the folded carbonate and sediment layers are much sharper and less distorted after FWI.

Fault Constrained Tomography

The CIG S/N ratio is quite low within fault shadows if the data is migrated with a smooth initial velocity. Residual curvature picking is very challenging, but it's also very critical for tomography to give correct updates. With broadband data, the low frequency reflections have better penetration and less distortion. Therefore more reliable residual curvature can be picked for tomography using this broadband dataset.

The initial velocity model may contain large errors in the area around the faults. Conventional tomography is not able to identify the large velocity errors, due to the internal regularization used to stabilize the inversion (Zhou et al., 2003). FCT (Birdus, 2007) updates the velocity only near the fault planes and tries to restore the velocity contrast across the fault.

In this new case study, the fault was used to constrain the tomography regularization. Major faults were still supplied to the tomography, together with residual curvature picks. The velocity update was not limited to near fault planes but was done for the entire model. The internal tomographic regularization was modified to honor the velocity contrast across the faults.

The result after three standard tomographic iterations is shown on Figure 4 (left). An interval velocity model in depth with good horizontal and vertical resolution has been achieved, but a strong fault shadow can still be seen in the corresponding PSDM image. On Figure 4 (right), several major faults are picked and used in FCT, and as a result the velocity model has better resolution across the fault. In the corresponding PSDM image, the fault shadow effect is reduced, and even secondary faults beneath the major fault are clearly imaged.

Discussions

Various techniques have been tested in this case study to solve the fault shadow distortion from shallow to deep: we formulate the following observations for this project, and also simplify them into a sketch on Figure 5.

- For the shallow water area down to 500 m depth, diving wave tomography gives a reasonable update and can tolerate moderate S/N ratio when the first breaks are clear. But diving wave tomography did not update as deeply as would have been expected from the actual diving wave depth of penetration, probably because the first break time only was not enough for this complex, under-determined problem.
- FWI makes use of the full waveform information, so it can update from water bottom down to about 2000 m even with even very low S/N ratio data.
- High-resolution reflection tomography with little internal regularization is able to solve the mild fault shadow from 500 m beneath the sea surface to 1500 m beneath the water bottom, if the CIG quality is good.
- FCT extends the ability to update down to about 4000 m beneath the water bottom. FCT tolerates moderate S/N ratio CIGs within the fault shadow because it can use a larger internal regularization to stabilize the inversion, but still keeps the velocity contrast sharp across the fault.

In general, reasonable geological constraints are always useful and sometimes are the only guide in the case of very low S/N ratio.

Results and Conclusions

DOI http://dx.doi.org/10.1190/segam2015-5841904.1

The PSTM image is stretched to the depth domain with a smooth depth-velocity function for comparison with the PSDM image on Figure 6. It is clear that, with a velocity model built from FWI and FCT, the PSDM image shows significant improvement compared to PSTM in this sub-thrust geological situation. The PSDM image provides better-focused events and more realistic geological structures, which are distorted in the PSTM image. This will help to reduce the structural uncertainty, particularly in the deeper section, and allow a better understanding of the petroleum system of this frontier exploration target.

Fault shadows have always been a challenging problem, especially in sub-thrust areas. In this case study, broadband seismic, FWI, and FCT played the most important role in addressing this problem.

Acknowledgements

The authors thank INPEX, Pertamina Hulu Energi, SKKMIGAS, MIGAS and CGG for the permissions to publish the paper. Also we would like to thank the other processing and QC team members for their great effort.

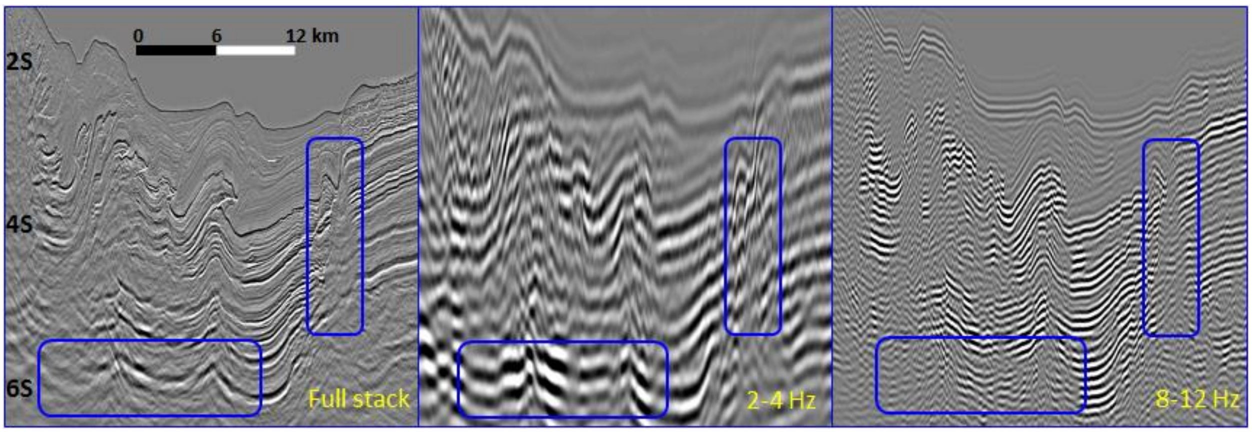

Figure 2: PSTM of the broadband seismic data comparing the full stack with the indicated frequency panels.

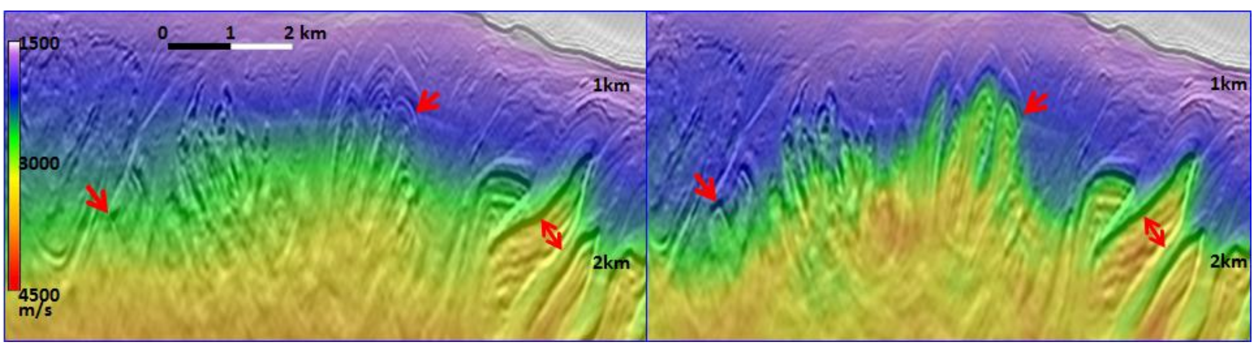

Figure 3: Left: velocity and corresponding PSDM stack after three tomographic iterations used as the input to FWI, and right: after FWI.

DOI http://dx.doi.org/10.1190/segam2015-5841904.1

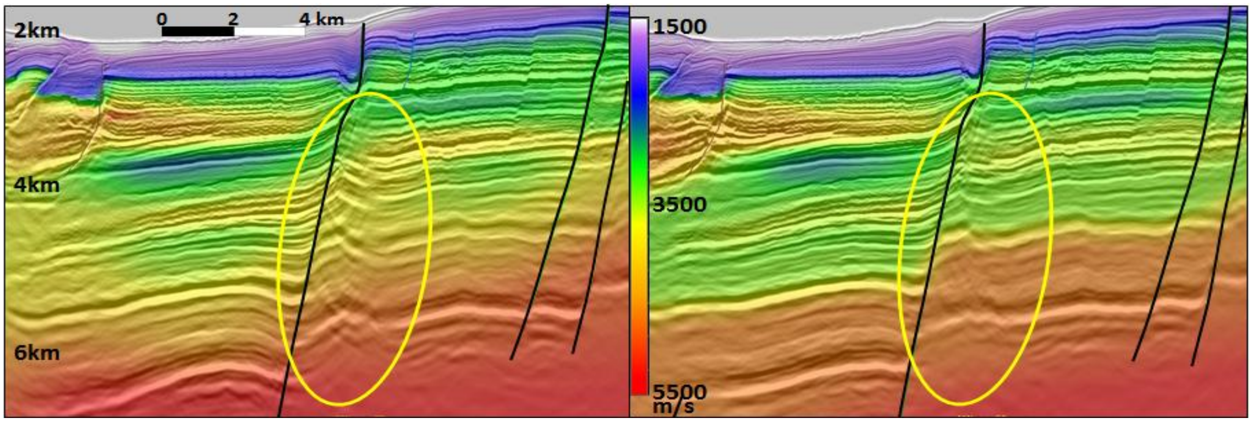

Figure 4: PSDM stack and overlaid velocity across the fault. Left: before FCT, right: after FCT.

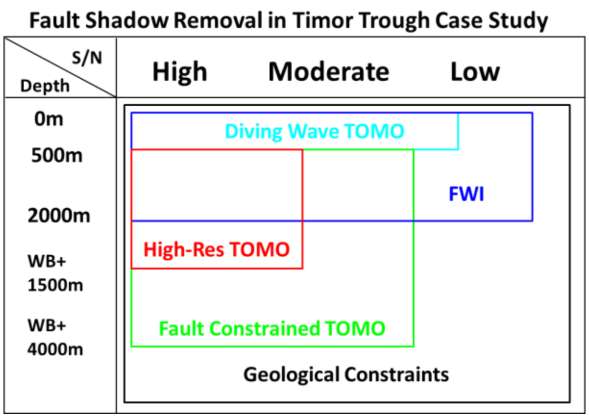

Figure 5: Applicable methods for fault shadow removal at different depth and with different CIG S/N ratio, based on this case study.

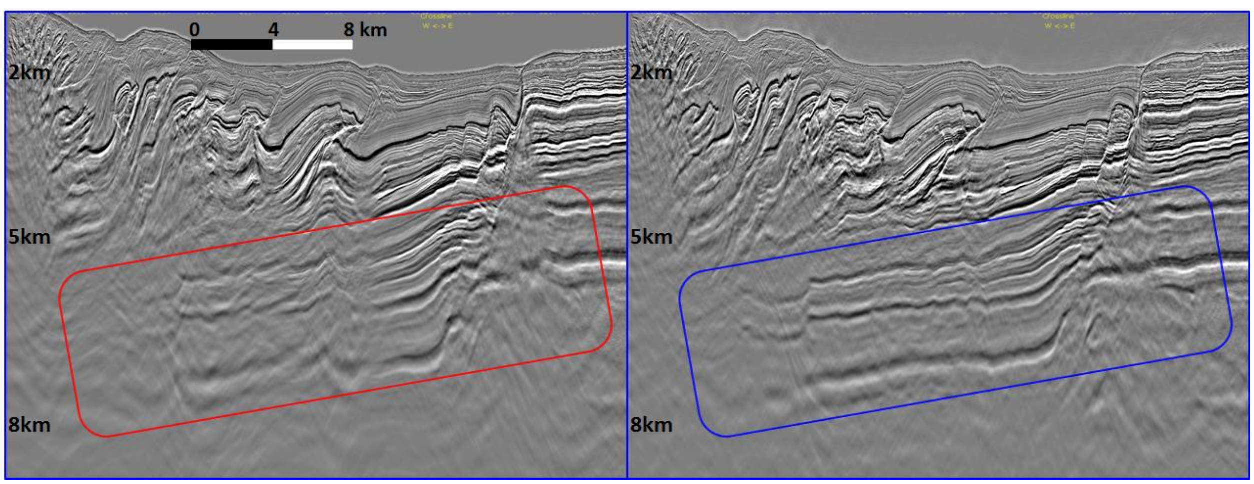

Figure 6: Left: PSTM stack stretched to depth, and right: PSDM stack obtained with final velocity model. The deep target area is highlighted.

EDITED REFERENCES
Note: This reference list is a copyedited version of the reference list submitted by the author. Reference lists for the 2015 SEG Technical Program Expanded Abstracts have been copyedited so that references provided with the online metadata for each paper will achieve a high degree of linking to cited sources that appear on the Web.

REFERENCES

Birdus, S., 2007, Removing fault shadow distortions by fault constrained tomography: 77th Annual international Meeting, SEG, Expanded Abstracts, 3039–3043.

Soubaras, R., and R. Dowle, 2010, Variable-depth streamer — A broadband marine solution: First Break, **28**, no. 12, 89–96.

Wang, P., and C. Peng, 2013, Premigration deghosting for marine streamer data using a bootstrap approach in Tau-P domain: 83rd Annual International Meeting, SEG, Expanded Abstracts, 4221–4225.

Zhou, H., S. H. Gray, J. Young, D. Pham, and Y. Zhang, 2003, Tomographic residual curvature analysis: The process and its components: 73rd Annual international Meeting, SEG, Expanded Abstracts, 666–669.